Virology 460-461 (2014) 11–22

Contents lists available at ScienceDirect

Virology

journal homepage: www.elsevier.com/locate/yviro

Ubiquitination and degradation of the ORF34 gene product of equine herpesvirus type 1 (EHV-1) at late times of infection

Abdelrahman Said [a,b], Armando Damiani [a], Nikolaus Osterrieder [a,*]

[a] Institut für Virologie, Zentrum für Infektionsmedizin—Robert von Ostertag-Haus, Freie Universität Berlin, Robert-von-Ostertag-Str. 7-13, 14163 Berlin, Germany
[b] Parasitology and Animal Diseases Department, National Research Center, Dokki, Giza, Egypt

ARTICLE INFO

Article history:
Received 18 February 2014
Returned to author for revisions
21 March 2014
Accepted 7 May 2014
Available online 29 May 2014

Keywords:
EHV-1
ORF34 gene
Protein degradation

ABSTRACT

The equine herpesvirus type 1 (EHV-1) open reading frame 34 (ORF34) is predicted to encode a polypeptide of 161 amino acids. We show that an ORF34 deletion mutant exhibited a significant growth defect in equine peripheral blood mononuclear cells taken directly *ex vivo* during early but not late times of infection. ORF34 protein (pORF34)-specific antibodies specifically reacted with a 28-kDa early polypeptide present in the cytosol of infected cells. From 10 h post infection, multiple smaller pORF34-specific protein moieties were detected indicating that expression of a late viral gene product(s) caused pORF34 degradation. Proteasome inhibitors blocked pORF34 degradation as did treatment of infected cells with a ubiquitin-activating enzyme (E1) inhibitor. Finally, kinetic studies showed that pORF34 is modified by addition of multiple copies of ubiquitin. Taken together, our findings suggest that the ubiquitin proteasome pathway is required for pORF34 degradation that may modulate protein activity in the course of infection.

Introduction

Equine herpesvirus type 1 (EHV-1) is a member of the genus *Varicellovirus* within the *Alphaherpesvirinae* subfamily (Davison et al., 2009) and remains one of the most common viral infections of horses causing respiratory, neurological and abortigenic disease (Allen et al., 2004; Allen and Yeargan, 1987; Carroll and Westbury, 1985; Crabb and Studdert, 1995). Its genome is a double-stranded DNA of 150-kbp in length (Nugent et al., 2006; O'Callaghan and Osterrieder, 2008) with 80 identified open reading frames (ORFs) that encode 76 unique genes and 4 that are duplicated in the inverted repeat regions (Davison et al., 2009; Telford et al., 1992). Viral replication requires a coordinated gene expression program in which immediate early (IE) progresses to early (E) and finally late (L) gene expression (Caughman et al., 1985; Gray et al., 1987). *Alphaherpesvirus* genomes exhibit a generally colinear gene arrangement and most of the genes are conserved among the different members of the subfamily. Exceptions to this rule apply to six of the 76 unique genes in EHV-1, namely ORF 1, 2, 3, 34, 59 and 67, which do not have known homologues in human herpes simplex virus (HSV) (Telford et al., 1992). The ORF1, 2, 3, 59 and 67 gene products of EHV-1 have already been characterized previously (Ma et al., 2012; Soboll Hussey et al., 2011; Ahn et al., 2011; Osterrieder et al., 1996; Said and Osterrieder, 2013). EHV-1 ORF34 and its product have not yet been characterized. The gene is located in the unique-long region of the genome and predicted to encode a protein with a calculated molecular mass of approx. 18,000 (Telford et al., 1992). Alignment by CLUSTAL of the amino acid sequence of EHV-1pORF34 to its counterparts of EHV-4 (pORF34) and VZV (pORF32) revealed that EHV-1pORF34 has an overall amino acid identity of 72% with its EHV-4 counterpart but only 24% with VZV pORF32 (Fig. 1).

Herpesvirus replication requires extensive modulation of many cellular pathways, among them the ubiquitin–proteasome pathway. For example, the HSV-1 transactivator ICP0 has been shown to utilize the proteasome-dependent pathway to induce cellular protein degradation and steer viral replication (Boutell et al., 2002; Everett, 2000; Kalejta and Shenk, 2003). The ubiquitin–proteasome system regulates important cellular functions including the cell cycle, antigen presentation, signal transduction and gene transcription as well as DNA repair (Pickart and Fushman, 2004; Prosch et al., 2003). The activation of ubiquitin by the E1 ubiquitin-activating enzyme, followed by the covalent addition of ubiquitin onto substrates by a number of ubiquitin ligases results in either protein degradation or modification of protein function (Pickart and Fushman, 2004; Prosch et al., 2003). Proteins tagged for degradation are targeted to the 26S proteasome, a multimeric protease consisting of a 20S catalytic core capped at both ends by 19S regulatory subunits (Demartino and Gillette, 2007; Forster and Hill, 2003). Cells utilize the proteasomal pathway to tune protein

* Corresponding author. Tel.: +49 30 838 51822; fax: +49 30 838 451822.
E-mail address: no34@cornell.edu (N. Osterrieder).

http://dx.doi.org/10.1016/j.virol.2014.05.009
0042-6822/

Fig. 1. CLUSTAL alignment of the EHV-1 pORF34 with its orthologues of EHV-4 and VZV. Amino acid residues that are conserved in the three proteins are shown in black boxes. The EHV-1 pORF34 has 72% and 24% overall amino acid identity with its orthologues of EHV-4 and VZV, respectively.

levels and efficiently degrade aberrantly folded proteins to ensure cellular homeostasis.

Considerable effort has been devoted to understanding the replication of EHV-1 and the function of its gene products in order to generate information that may be useful in the rational design of better vaccines. To date, the product of EHV-1 ORF34 is a viral protein with unknown function. The goals of this study were to identify and characterize the EHV-1 ORF34 gene product and to investigate whether the ORF34 protein (pORF34) has a role in virus replication. We, therefore, generated and characterized an EHV-1 Ab4 mutant with a deletion of ORF34 and report that EHV-1 ORF34 is expressed with early kinetics and its product is localized within the cytosol of infected cells. In addition, pORF34 is degraded in the proteasome following ubiquitination, a process that requires a late viral gene product(s). Moreover, EHV-1 Ab4 ORF34 expression replicated with reduced efficiency *in vitro* at early but not late stages of infection.

Results

Generation of mutant viruses

To generate EHV-1 Ab4 lacking ORF34 (rAb4Δ34), *en passant* mutagenesis was employed (Fig. 2A) (Tischer et al., 2006). During the first recombination event, the insertion into pAb4 of the amplified *aphA1* gene instead of ORF34 gene resulted in kanamycin-resistant intermediates that exhibited the expected changes as reflected in the *XbaI* restriction enzyme pattern by the presence of a fragment of 9749 bp in size compared to the 8719 bp fragment present in pAb4 (Fig. 2B). Positive clones were subjected to the second round of Red recombination to obtain the final construct after excision of the *aph*AI gene (Tischer et al., 2006). DNA from colonies that were kanamycin-sensitive but chloramphenicol-resistant was extracted and again checked by RFLP analysis after digestion with *XbaI*. The second recombination event resulted in the reduction in size of the 9749 bp *XbaI* fragment to 8236 bp (Fig. 2B). The results of the RFLP analysis were confirmed by Southern blotting, which revealed that only the *XbaI* band containing ORF34 sequences in pAb4 and the pAb4Δ34R revertant clone, but not that in pAb4Δ34, was reactive with the ORF34-specific probe (data not shown). Nucleotide sequencing further confirmed the deletion of ORF34 in the mutant pAb4Δ34.

Next, a virus with an HA-tag at the C-terminus of ORF34 was generated using the same methodology. PCR analysis showed that HA tag sequences in pAb4_34-HA were correctly inserted, which was confirmed by nucleotide sequencing (data not shown) and RFLP (Fig. 2). In the pAb4_34-HA intermediate, the 8719 bp *XbaI* fragment present in pAb4 increased in size to 9724 bp. After the second recombination and removal of the *aphA1* gene, a reduction in size of the 9724 bp *XbaI* fragment to 8746 bp was evident (Fig. 2C). The appropriate revertant from pAb4Δ34, in which the original sequences were restored, was also generated using *en passant* recombination (Fig. 2).

In vitro characterization of the ORF34 protein

To characterize the ORF34 product, recombinant EHV-1 with an HA tag at the C-terminus of ORF34 (rAb4_34-HA) as well as a polyclonal anti-pORF34 antibody targeting the protein's N-terminus (N-pORF34) were used. To verify the specificity of the anti-HA MAb in the detection of pORF34 expression, RK13 cells were transfected with expression vectors harboring either ORF34 (pcDNA_34) or ORF34 tagged with HA sequences (pcDNA_34-HA). Also, lysates of RK13 cells infected with parental rAb4 or rAb4_34-HA were included in the assay. Cell lysates were harvested from transfected and infected cells and subjected to Western blot analysis using the anti-HA MAb and the N-pORF34 antibody. In transfected cells, the anti-HA antibody detected a 28-kDa band corresponding to pORF34 in pcDNA_34-HA-transfected cells (Fig. 3A) but not in lysates of cells transfected with pcDNA (vector control) or pcDNA_34. The anti-HA antibody also detected a pORF34-specific band of the same size in rAb4_34-HA-infected cells at 5 h p.i., while multiple additional bands of 17- to 28-kDa were also detected at 24 h p.i. (Fig. 3B). Expression of pORF34 was not detected in the parental virus with the HA antibody (Fig. 3B). In contrast, the N-pORF34 antibody was able to detect only a single 28-kDa band in lysates of parental virus at 5 and 24 h p.i., but did not react with the additional bands of 17- to 28-kDa at 24 h p.i. (Fig. 3C). We concluded from the results that both the anti-HA antibody and the pORF34-specific peptide antibody were able to detect a 28-kDa pORF34-specific band and did not exhibit any cross-reactivity with other viral or cellular proteins.

pORF34 is expressed with early kinetics and is not post-translationally modified by phosphorylation or glycosylation

To determine the kinetics of ORF34 expression, Western blot analysis was performed with lysates of infected cells harvested at different time points in the presence or absence of PAA. Expression of β-actin and gM, a late EHV-1 protein, was also assessed to control efficiency of PAA treatment. The HA-tagged pORF34 was detected as early as 1 h p.i. at significant levels, which was not affected by PAA treatment, in contrast to gM expression (Fig. 4A). To clearly distinguish between the IE or E phase of gene expression, NBL6 cells were either mock-infected or infected with rAb4_34-HA in the presence of CX for 5 h followed by extensive washing and addition of Act-D (CX/Act-D), and treated cells were

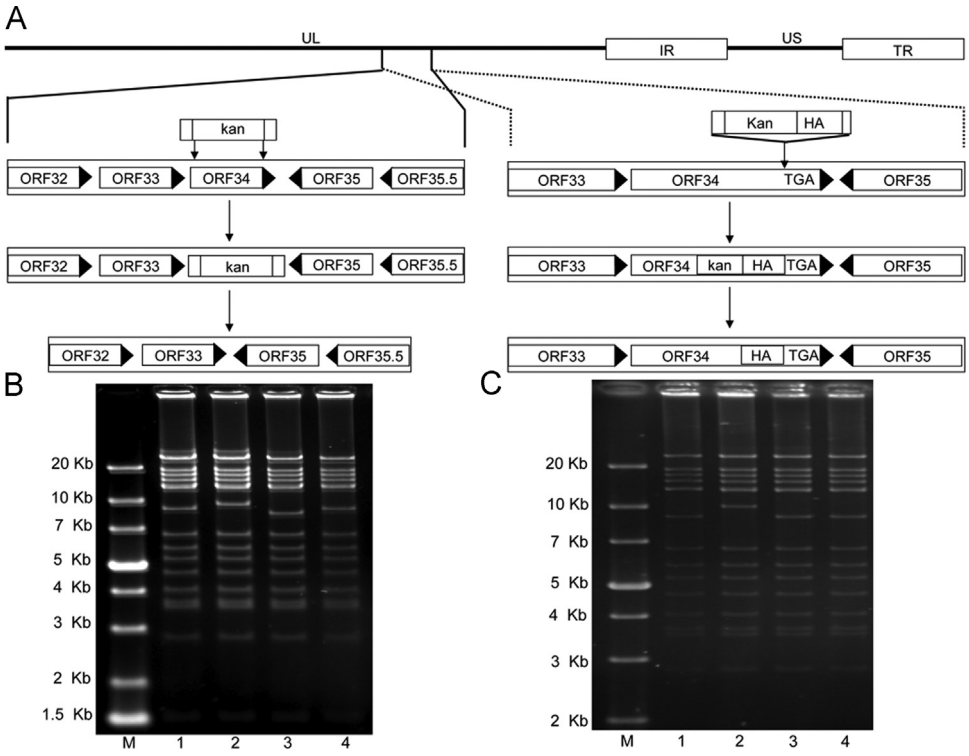

Fig. 2. Construction of EHV-1 lacking ORF34 (rAb4Δ34) or expressing epitope-tagged pORF34 (rAb4_34-HA). (A) Schematic diagram of the procedures used to delete the ORF34 gene from pAb4 and to insert an HA tag at the pORF34 carboxy-terminus. Schematic representation of the genomic organization and the *XbaI* restriction map of (pAb4) is given. The two unique segments (UL and US), and the terminal and internal repeat sequences (TRS and IRS) are shown. Two-step *en passant* mutagenesis was employed for manipulation of pAb4 and for generation of rAb4Δ34 and rAb4_34-HA. (B) Identification of pAb4Δ34 by RFLP. Purified DNA from pAb4 (lane 1), the kanamycin-resistant intermediate (lane 2), the final constructs pAb4Δ34 (lane 3) and pAb4Δ34R (lane 4) were digested with *XbaI* and separated by 0.8% agarose gel electrophoresis. (C) Identification of pAb4_34-HA by RFLP. Purified DNA from pAb4 (lane 1), the kanamycin-resistant intermediate (lane 2), the final mutant pAb4_34-HA (lane 3) and pAb4_34-HAR (lane 4) were digested with *XbaI* and separated by 0.8% agarose gel electrophoresis. GeneRuler 1 kb Plus DNA Ladder (Thermo Scientific) was used for determination of DNA fragment sizes and was loaded in lane M.

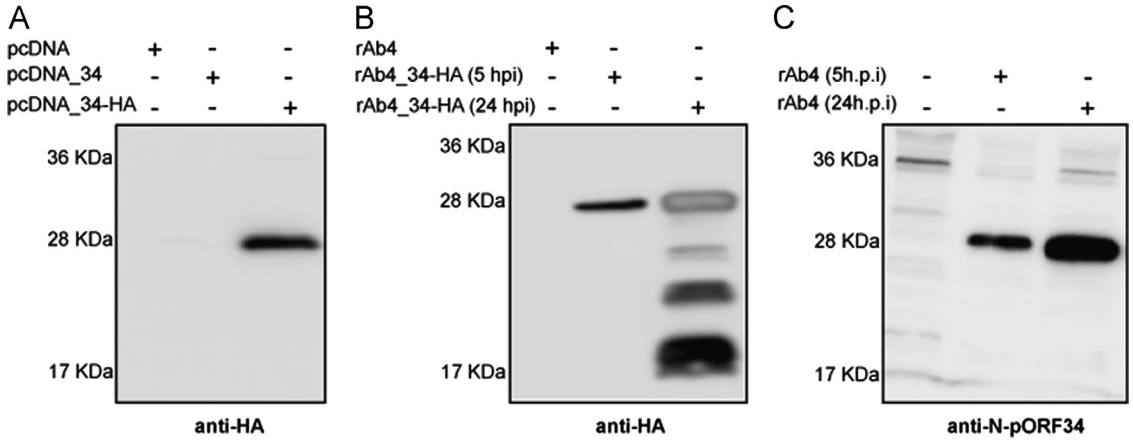

Fig. 3. Characterization of pORF34 expression in transfected or infected cells. (A) RK13 cells were transfected with either pcDNA, pcDNA_34 or pcDNA_34-HA. A 28-kDa band was detected in cell lysates transfected with pcDNA_34-HA but not in those pcDNA and pcDNA_34. Cells were infected either with parental rAb4 or rAb4_34-HA (B) or parental rAb4 virus (C). At different times after infection (5 and 24 h p.i.), cell lysates were prepared and subjected to Western blot analysis. Anti-HA antibody or anti-pORF34 peptide antibody were used to detect pORF34 expression in (B) and (C), respectively. Identical concentrations of protein lysates were separated in each lane of an SDS-12% polyacrylamide gel. The PageRulerTM Prestained protein ladder (Thermo Scientific) was used for determination of protein sizes.

subjected to Western blot analysis (Fig. 4B). pORF34 was not detected after treatment of cells with CX/Act-D (Fig. 4B). Taken together, we concluded that pORF34 is expressed with early kinetics in infected cells. It was previously reported that VZV pORF32 was modified by phosphorylation (Reddy et al., 1998). To test the hypothesis that the EHV-1 orthologue is also modified by phosphorylation, rAb4_34-HA-infected cell lysates were treated with λ-PPase. We were unable to demonstrate any change in electrophoretic mobility of any of the pORF34 moieties in the presence of the enzyme (data not shown). To determine whether EHV-1 protein kinases, encoded by US3 (ORF69) and UL13 (ORF49) might be associated with the phosphorylation of pORF34, NBL6 cells were infected with the respective protein kinase mutants (Ma et al., 2012). Multiple forms of pORF34 were still detected by Western blot analyses in cells after infection with either of the mutants (data not shown). Furthermore, to address pORF34 modification by glycosylation, rAb4-infected cell lysates were treated with either PNGaseF or EndoH. Using anti-pORF34

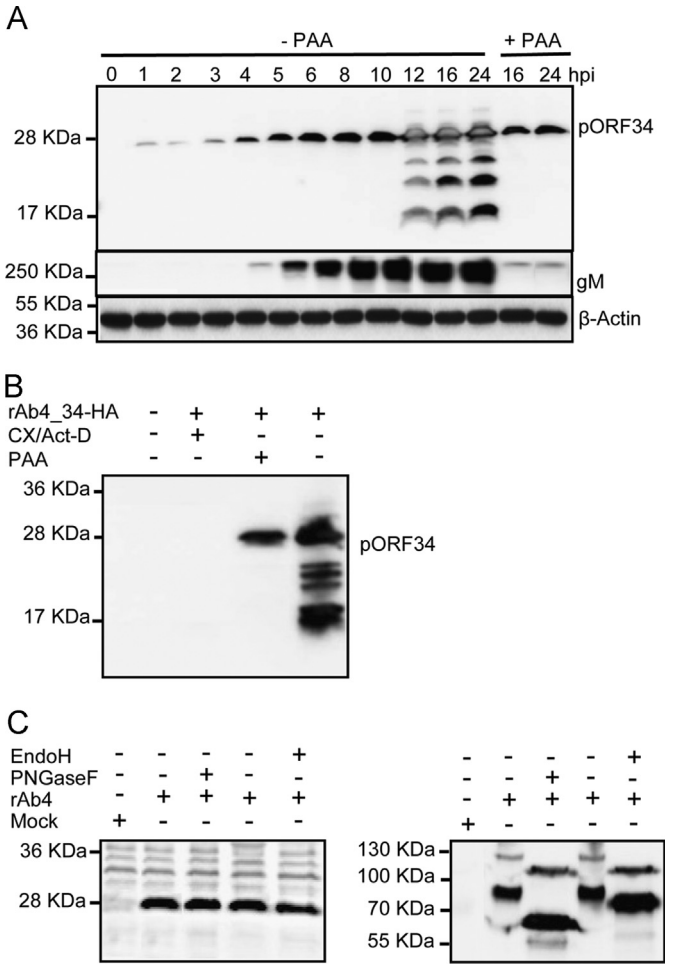

Fig. 4. pORF34 is expressed with early kinetics and is not glycosylated. (A) Expression of pORF34 in the presence or absence of PAA was determined for each time point in panel A by Western blotting. Proteins were extracted from RK13 cells infected with rAb4_34-HA and an anti-HA MAb was used for detection. A 28-kDa band was detected at 1 to 12 h p.i., as well as 16 and 24 h p.i. in the presence of PAA. Bands with apparent molecular weights between 17- and 28-kDa were detected at 12, 16, and 24 h p.i. in the absence of PAA. Expression of gM and β-actin was determined as controls. (B) To differentiate whether pORF34 is an early or immediate early protein, lysates from mock-infected cells or cells infected with rAb4_34HA in the presence or absence of CX/Act-D were prepared and analyzed by immunoblotting. A band of 28-kDa in size was detected in the presence of PAA (Lane 4), and the 17-to 28-kDa moieties were detected in the absence of PAA. (C) RK13 cells were either mock-infected or infected with rAb4 virus. Cell lysates treated with PNGaseF or EndoH (BioLabs) for 3 h at 37 °C were analyzed by Western blotting. Expression of gB, a glycosylated protein, was used as control for the efficiency of PNGaseF and EndoH treatment. The PageRulerTM Prestained protein ladder (Thermo Scientific) was used for determination of protein molecular masses.

antibody targeting the protein's C-terminus (C-pORF34), we were unable to detect any such modifications of pORF34 (Fig. 4C, left panel). Expression of gB was used as a control for the efficiency of PNGaseF or EndoH treatment (Fig. 4C, right panel). Taken together, we concluded from our results that pORF34 is not posttranslationally modified by glycosylation or phosphorylation.

pORF34 degradation is time-dependent

We had observed that multiple pORF34-specific bands were detectable at later times after infection with the anti-HA antibody that targeted the HA tag inserted at the C-terminus of the protein in the rAb4_34-HA virus. However, only the full-length 28-kDa band was detected with the anti-N-pORF34 antibody in rAb4 or rAb4_34-HA at all times p.i. These results strongly suggested the protein may undergo degradation. In order to assess the rate of the presumed pORF34 degradation, RK13 cells were infected with rAb4_34-HA virus. Infected cells were harvested at various times p.i. (1, 2, 3, 4, 5, 6, 8, 10, 12, 16 and 24) and analyzed by immunoblot. We observed only one specific band of 28-KDa for pORF34 from 1 to 10 h p.i. At later times after infection, however, additional bands with apparent molecular masses ranging between 17- and 28-kDa appeared (Fig. 4A). Moreover, after treatment of infected cells with PAA at 16 and 24 h p.i., only the original 28-kDa pORF34-specific band was detected (Fig. 4A). Overall, our findings suggested that expression of a late viral protein(s) has a direct or indirect role in the appearance of multiple pORF34 species.

pORF34 undergoes amino-terminal degradation

To determine whether EHV-1 ORF34 protein indeed undergoes (amino-terminal) degradation, RK13 cells were either mock-infected or infected with rAb4 or rAb4_34-HA. Cell lysates were harvested at 24 h p.i. from non-infected and infected cells and subjected to Western blot analysis using anti-HA MAb and antibodies targeting the N- and C-terminus of pORF34. All of the antibodies specifically reacted with a band of approximately 28-kDa in lysates of infected cells (Fig. 5). However, reactivity of the band was weaker in the case of the anti-C-pORF34 antibody in rAb4_34-HA-infected cell lysates (Fig. 5B). Furthermore, the anti-HA MAb and the polyclonal antibody targeting the C-terminus of pORF34 reacted with multiple smaller bands at later times p.i. In contrast, those smaller bands were not reactive with anti-N-pORF34 antibody in cells infected cells with either rAb4_34-HA or rAb4 (Fig. 5C). We concluded from these observations that the ORF34 protein undergoes degradation that is initiated at its N-terminus.

Degradation of pORF34 occurs through the ubiquitin/proteasome pathway

To examine the effect of the proteasomal degradation pathway on pORF34 processing, RK13 cells were either mock-infected or infected with rAb4_34-HA for 1 h to allow for virus adsorption. After adsorption, cells were incubated with fresh medium with or without lactacystin, a proteasome inhibitor, for an additional 24 h. Western blot analysis of cell lysates revealed the presence of a 28-kDa band in cells treated with lactacystin, while additional bands of 17- to 28-kDa were observed in non-treated cells, consistent with our earlier findings (Fig. 6A). We concluded that pORF34 is degraded through the proteasomal pathway.

In order to address whether pORF34 degradation through the proteasome was dependent on ubiquitination, RK13 cells were transfected with a 6XHis-tagged ubiquitin expression plasmid. At 24 h after transfection, cells were infected with the rAb4_34-HA virus for 24 h. Then, cell lysates were subjected to immunoprecipitation using the anti-HA or -His MAb on the same lysates. Coupling of ubiquitin to pORF34 was detected by reciprocal immunoblot analysis with anti-HA or anti-His antibodies, respectively. As suggested by the presence of multiple bands, pORF34 was modified by addition of multiple copies of ubiquitin (Fig. 6B). To confirm these results, RK13 cells were mock-infected or infected with rAb4_34-HA for 1 h followed by treatment with the E1 ligase inhibitor Pyr-41 for 24 h. Western blot analysis of Pyr-41-treated cells indicated that the pORF34-specific band was reduced in size but no degradation products were identified even at late times after infection (Fig. 6C).

Taken together, our results showed that pORF34 is ubiquitinated at later times after infection and targeted for degradation by the proteasome.

To address the extent of covalent ligation of ubiquitin molecules to pORF34, the viral protein was precipitated from cells infected with either rAb4 parental or rAb4_34HA virus using an

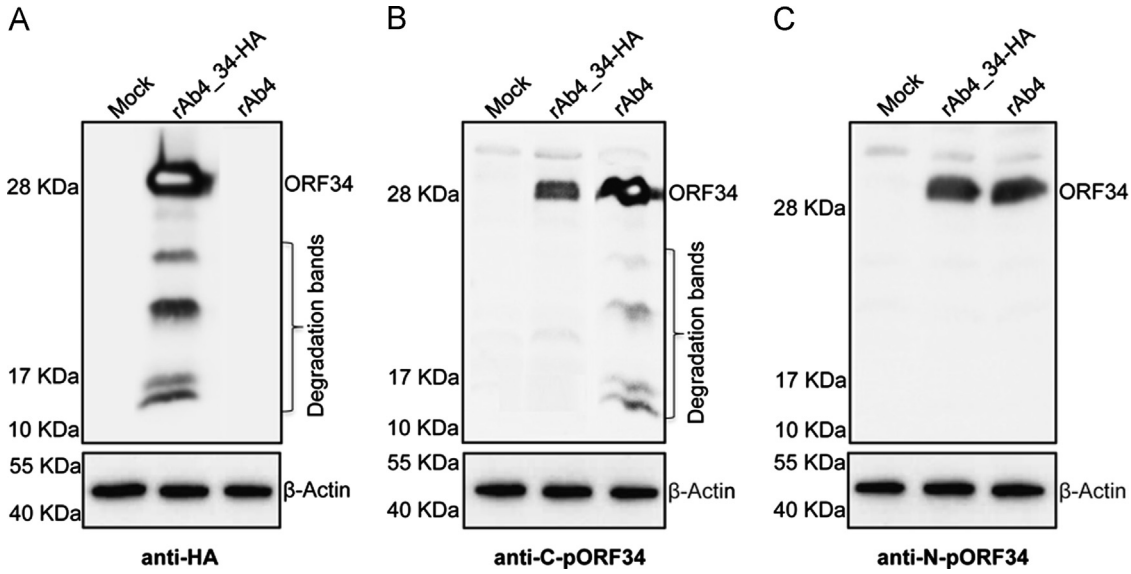

Fig. 5. Degradation of pORF34. To determine degradation of pORF34, RK13 cells were mock-infected or infected with either rAb4_34-HA or rAb4. Cell lysates were collected 24 h p.i. and then analyzed by Western blotting using anti-HA MAb (A) or anti-ORF34 peptide antibodies (B and C). All used antibodies reacted with a band of 28-kDa in cells infected with rAb4 and rAb4_34-HA. The 17-to 28-kDa bands were detected with anti-HA MAb and anti-C-pORF34 (panels A and B) antibodies, but were not detected with anti-N-pORF34 antibody (C). Prestained protein ladder (Thermo Scientific) was used for determination of protein molecular masses.

anti-mono- and -poly-ubiquitin MAb. Then, immunoprecipitates were examined by Western blotting, using the anti-HA and anti-C-pORF34 antibody, respectively. Multiple pORF34-specific bands were detected in the ubiquitin-specific precipitates in cells infected with rAb4 parental and rAb4_34HA, while those bands were absent from precipitates of mock-infected cells (Fig. 7A).

To determine the kinetics of pORF34 ubiquitination and whether degradation is coincident with covalent addition of polyubiquitin to the polypeptide, RK13 cells were infected with rAb4 virus. Infected cells were harvested at different times p.i. (2, 5, 10, 12 and 24). Anti-ubiquitin antibody was used to precipitate ubiquitinated pORF34 and precipitated proteins were analyzed as described earlier. We observed multiple ubiquitin-containing bands using the pORF34-specific antibody starting at 12 h p.i. and lasting throughout the observation period (Fig. 7B). Our findings, therefore, suggest that EHV-1 pORF34 is ubiquitiated and that its degradation starts at a time when covalent attachment of multiple copies of ubiquitin to pORF34 can be detected.

pORF34 is located in the cytoplasm of infected cells

In order to determine the subcellular localization of pORF34, NBL6 cells infected with rAb4, rAb4_34-HA or mutant rAb4Δ34 were analyzed by indirect IF using anti-HA MAb or the anti-pORF34 peptide antibody. Both antibodies revealed localization of the ORF34 protein in the cytosol of cells infected with rAb4_34-HA or parental rAb4 (Fig. 8A and B). As expected, the anti-HA MAb did not detect pORF34 in cells infected with either parental EHV-1 lacking the HA tag or the rAb4Δ34 mutant (Fig. 8A). To confirm the localization of pORF34, cytoplasmic and nuclear fractions were obtained from NBL6 cells infected with rAb4_34-HA and subjected to Western blot analysis using the anti-HA MAb. These experiments corroborated the findings of the IF analyses and showed cytoplasmic localization of pORF34 (Fig. 8C).

Growth properties of ORF34-negative viruses in cultured cells

To determine whether pORF34 is essential for EHV-1 replication *in vitro*, equine NBL6 cells were infected with either parental, mutant rAb4Δ34 or revertant virus, and plaques sizes were determined. The results showed that the rAb4Δ34 was able to grow on NBL6 cells with average plaque sizes that were not significantly ($p=0.29$ and $p=0.34$) different from those observed after infection with parental or revertant viruses (Fig. 9A). We concluded from the results that deletion of ORF34 is not required for efficient growth of EHV-1 in cultured fibroblasts. When mutant virus replication was evaluated by single-step growth kinetics, extracellular and cell-associated virus titers of rAb4Δ34 virus were determined at different time points. The EHV-1 ORF34 deletion mutant grew with titers lower than parental and revertant viruses at early times of infection (until 10 h p.i.). Starting from 12 h p.i., however, titers of mutant as well as parental and revertant virus were virtually identical (Fig. 9B). These findings suggest that the ORF34 protein is required for optimal replication of EHV-1 in cultured cells at early times of infection.

To evaluate whether deletion of ORF34 impairs virus replication in a compartment important for EHV-1 replication and pathogenesis *in vivo*, virus genome copies in equine PBMC infected with either rAb4Δ34 virus, parental or revertant viruses were determined by qPCR at 5 and 24 h p.i. All tested viruses were capable of infecting PBMC with similar efficiencies (data not shown). Significant differences in viral genome copies were detected at 5 but not at 24 h p.i. in that an approximately 7-fold reduction in rAb4Δ34-infected PBMC was recorded at that time point (Fig. 10). We concluded from our result that the ORF34 protein is required for optimal replication efficiency in equine PBMC at early stages of infection.

Discussion

The ORF34 product of EHV-1 was the focus of this study. Positional homologues to EHV-1 ORF34 have been identified in EHV-4 gene 34 (Telford et al., 1998) and VZV gene 32 (Reddy et al., 1998), but no homologous ORF was identified members of the *Simplexvirus* genus (McGeoch et al., 1988, 1991). The predicted VZV ORF32 and EHV-1/-4 ORF34 products are similar in length and have low isoelectric points (3.9 to 4.8), because at least 15% of each of the proteins is comprised of acidic amino acids. The VZV ORF32 protein has 24% overall amino acid identity with its EHV-1 and 72%

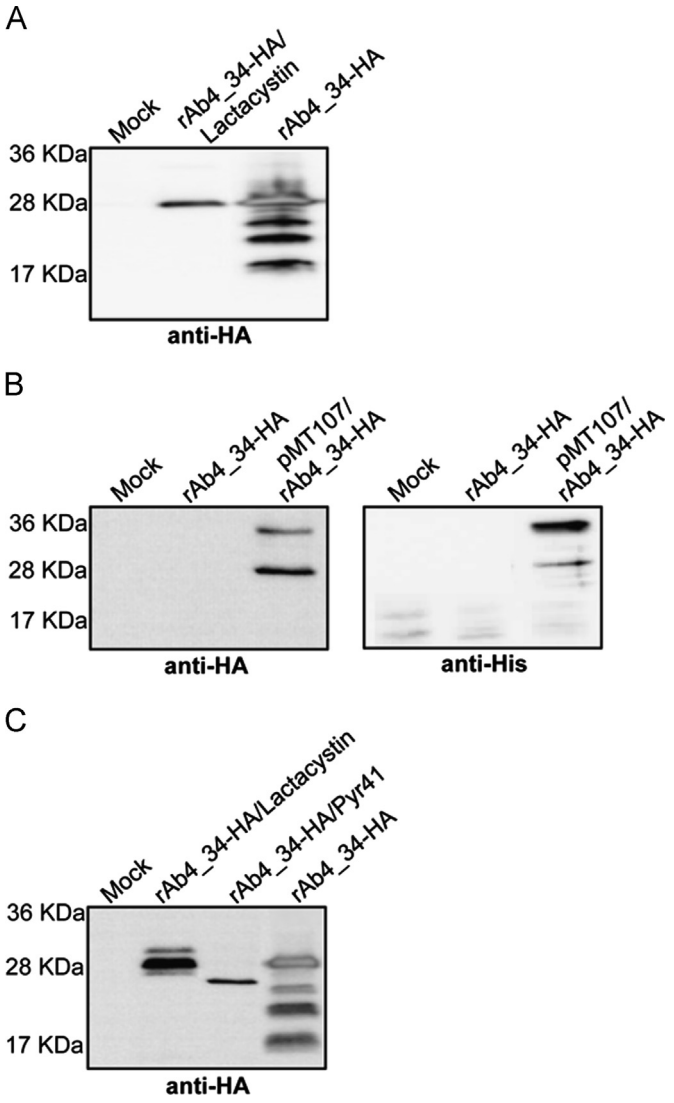

Fig. 6. pORF34 protein degradation is *via* the ubiquitin/proteasome pathway. (A) A proteasome inhibitor (lactacystin, 10 mM) was added to cells infected with rAb4_34-HA. The drug was left on the cells for 24 h at 37 °C. Treated cells were then collected and analyzed by Western blotting. Bands with molecular weights of 28-kDa or 17- to 28-kDa were detected with the anti-HA antibody in the presence and absence of lactacystine, respectively. (B) To investigate whether pORF34 is ubiquitinated, RK13 cells were mock-infected, infected with rAb4_34-HA or transfected with pMT107 and then infected with Ab4_34-HA. Cell lysates were subjected to immunoprecipitation using the anti-HA (right panel) or anti-His MAbs (left panel). Then, pORF34 ubiquitination was detected by Western blot using an anti-HA (left panel) or an anti-His (right panel) antibody. Bands of 28- and 36-kDa were detected with the anti-HA and anti-His antibody only in lysates of cells transfected with pMT107 and infected with Ab4_34-HA. (C) To determine whether proteasomal degradation of pORF34 is ubiquitin-dependent, RK13 cells infected with rAb4_34-HA were treated with the E1 inhibitor (Pyr-41 at 25 μM) prior to and after infection, then the treated cells were harvested and analyzed by Western blotting. Prestained protein ladder (Thermo Scientific) was used for determination of protein molecular masses.

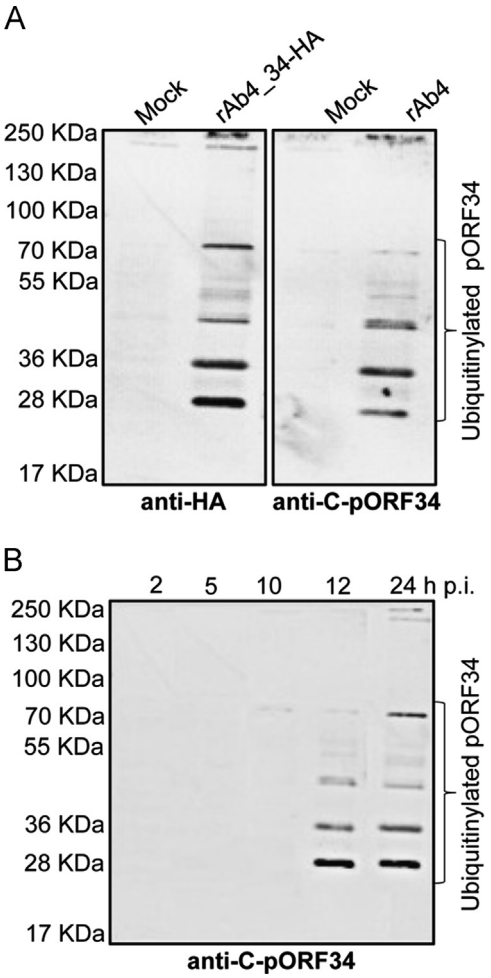

Fig. 7. Covalent attachment of ubiquitin to pORF34. (A) RK13 cells were either mock-infected (lanes 1 and 3), infected with rAb4_34HA (lane 2) or Ab4 parental virus (lane 4). Immunoprecipitation using anti-ubiquitin MAbs was performed and shown in the right and left panel, respectively. Samples were analyzed by Western blotting using anti-HA and anti-C-pORF34 antibody in the left and right panel, respectively. (B) Kinetics of ubiquitination of pORF34. Cells infected with rAb4 virus were harvested at 2, 5, 10, 12 and 24 h p.i. and treated with anti-Ub antibodies as described in (A). Precipitated proteins were subjected to SDS-12%–PAGE and analyzed by immunoblotting with anti-C-pORF34 peptide antibody. Prestained protein ladder (Thermo Scientific) was used for determination of protein molecular masses.

amino acid identity with the EHV-4 orthologue (48). Moreover, the three proteins are hydrophilic and none is predicted to be inserted into membranes.

For functional analysis of EHV-1 pORF34, kinetic studies of protein expression were conducted. Our data show that pORF34 expression started at 1 h p.i. and was not affected by PAA, indicating that pORF34 is an early viral protein. Our findings are in agreement with previous results showing that the VZV ORF32 protein is also expressed at early times after infection (Reddy et al., 1998). pORF34 (with the inserted HA epitope) is a protein with a molecular weight of 28-kDa in transfected and infected cells. Using anti-pORF34 antibodies targeting N- or C-terminal sequences of the protein, we detected a band with the same apparent molecular mass of 28-kDa. This apparent mass is larger than that predicted based on the sequence of the protein (18-kDa). Additional immunoblot analyses of pORF34 utilizing the anti-HA MAb and the anti-peptide antibody targeting the protein's C-terminus allowed specific detection of at least four bands ranging in molecular weight from 17- to 28-kDa later in infection. Notably, these lower molecular mass bands were detectable using the antibody targeting the C-terminus of pORF34 but we failed to detect the additional bands using the pORF34-specific antibody that was raised to a peptide located at the extreme N-terminus of the protein. Although we were able to detect the 28-kDa moiety using the anti-C-pORF34 antibody in cells infected with rAb4_34HA, we were not able to detect the additional (degradation) bands ranging from 17- to 28-kDa. This is an unexpected result, which offers room for speculation. We can think of two possible explanations, which both have to do with the insertion of the HA epitope and addition of 9 amino acids (YPYDVPDYA) at the C-terminus of pORF34. This addition may indeed have an effect on the

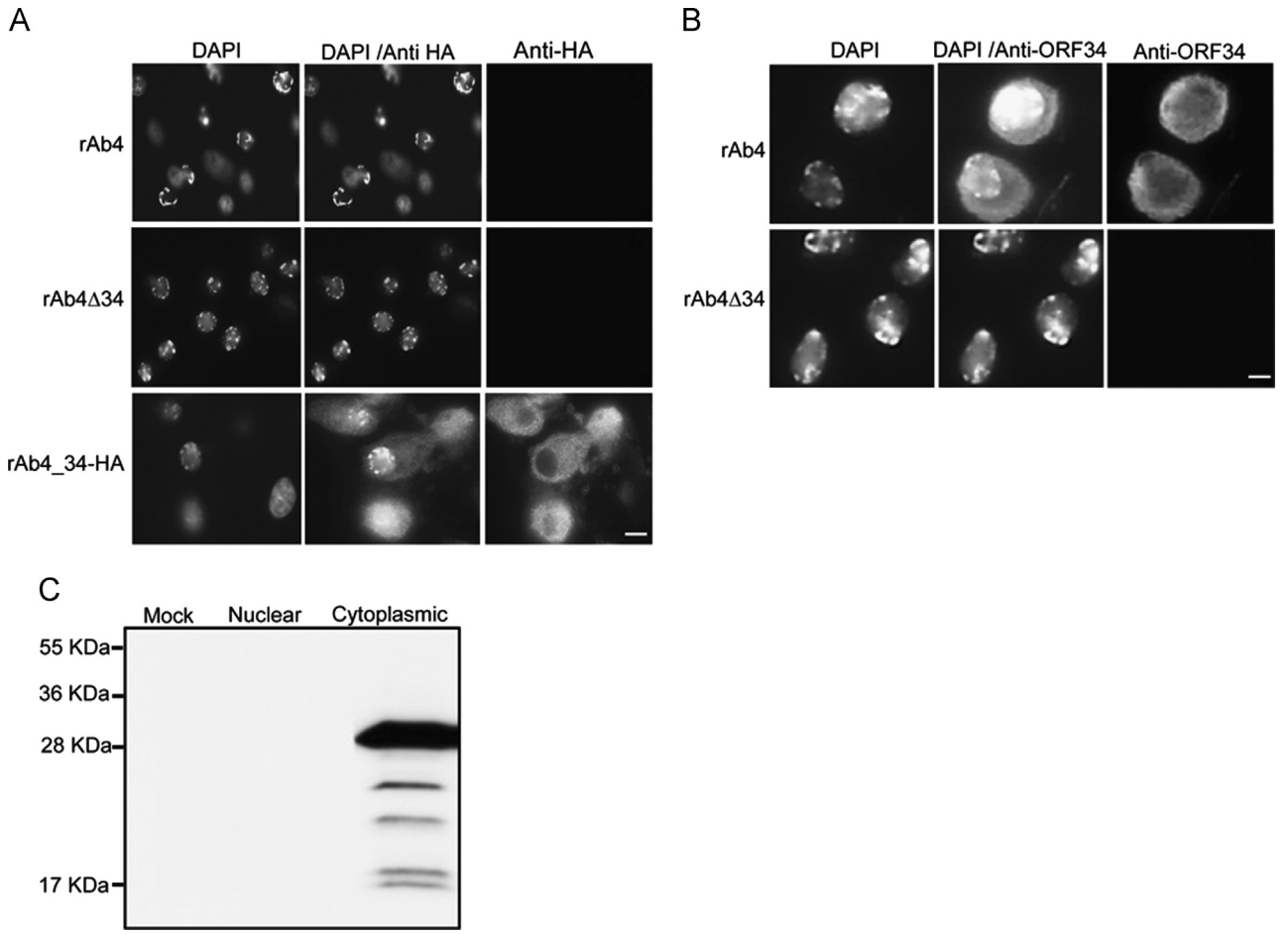

Fig. 8. Localization of p ORF34 in infected cells by immunofluorescence and Western blot analysis of subcellular fractions. For immunofluorescence, NBL6 cells were infected with either parental rAb4, rAb4_34-HA or rAb4Δ34 virus. At 16 h p.i., cells were fixed with 2% paraformaldehyde for 10 min and permeabilized with 0.1% saponin in PBS for 30 min. Monoclonal anti-HA and polyclonal Anti-ORF34 antibody were used as a primary antibody in (A) and (B), respectively, while Alexa Fluor 568 goat anti-mouse and Alexa Fluor 488 goat anti-rabbit IgG were used as secondary antibodies. Coverslips were mounted in a VECTASHIED® mounting medium with DAPI (Vector Laboratories) to stain nuclei. Magnification: 40×, scale bar=10 μm. (C) For cell fractionation, NBL6 cells were infected with rAb4_34-HA for 24 h or mock-infected, then cell lysates were separated into cytoplasmic and nuclear fractions before immunoblot analysis. Identical amounts of the protein were separated in each lane of an SDS-12% polyacrylamide gel and an anti-HA MAb was used for detection. pORF34 was not detected in the nuclear fraction (lane 2) but only the cytoplasmic fraction (lane 3). Prestained protein ladder (Thermo Scientific) was used for determination of protein molecular masses.

degradation process by increasing stability and reduced degradation that can only be visualized with the highly affine HA antibody. The other explanation that we favor is that addition of the epitope may interfere with binding of the anti-C-pORF34 antibody. Based on the data and the differential banding patterns detected with the anti-HA MAb and the pORF34-specific antibodies raised against peptides at the N- and C-terminus, we currently conclude that pORF34 is degraded sequentially from its amino-terminus.

We had originally surmised that the different bands may represent degradation products or different forms of the proteins due to posttranslational modifications. Phosphorylation is one of common posttranslational modification that regulates the herpesvirus protein function (McDowell et al., 2013; Oster et al., 2008; Reddy et al., 1998). We tested whether phosphorylation is responsible for the observed effect on EHV-1 pORF34 based on the fact that the VZV orthologue of pORF34 (VZV pORF32) is a phosphoprotein (Reddy et al., 1998) but could not confirm phosphorylation of the EHV-1 protein. Theoretically, glycosylation was also a possibility and we used enzymatic digestion with PNGaseF and EndoH to formally exclude that glycosylation is responsible for the posttranslational modification of the EHV-1 ORF34 protein.

Modification of proteins by covalent attachment of ubiquitin or ubiquitin-related polypeptides and the degradation of the conjugates by the proteasome participate in the regulation of fundamental cellular processes (Bregegere et al., 2006; Dye and Schulman, 2007; Hershko and Ciechanover, 1998). It is therefore not surprising that many pathogens have devoted a considerable part of their genomes to the production of proteins that mimic, block or redirect the activity of the ubiquitin–proteasome system in order to modify the cellular environment and protect infected cells from the host's immune attack. Our experiments with proteasome and E1 inhibitors provided insights into the mechanism of pORF34 degradation. Treatment with a proteasome inhibitor resulted in the inhibition of pORF34 degradation in cells infected with rAb4_34-HA. Proteasome-dependent protein degradation is usually contingent upon ubiquitination of proteins. Polyubiquitin is conjugated to target proteins through a process involving E1 ubiquitin-activating enzymes, E2 ubiquitin conjugating enzymes, and E3 ubiquitin ligases (Hershko and Ciechanover, 1998). It is worthwhile noting that the E1 inhibitor controls the biological activity of the ubiquitin E1 and, hence, blocks protein degradation (Teale et al., 2009; Yang et al., 2007). Therefore, incubation of infected cells with E1 inhibitors inhibited pORF34 degradation in cells infected with rAb4_34-HA. On the other hand, the size of pORF34 was reduced after treatment of infected cells with E1 inhibitors, suggesting that the ORF34 protein is indeed modified by addition of mono- or polyubiquitin. Interestingly, the kinetics of pORF34 expression had shown protein stability until 10 h p.i. We also noted that the apparent molecular mass of pORF34 of 28-kDa as

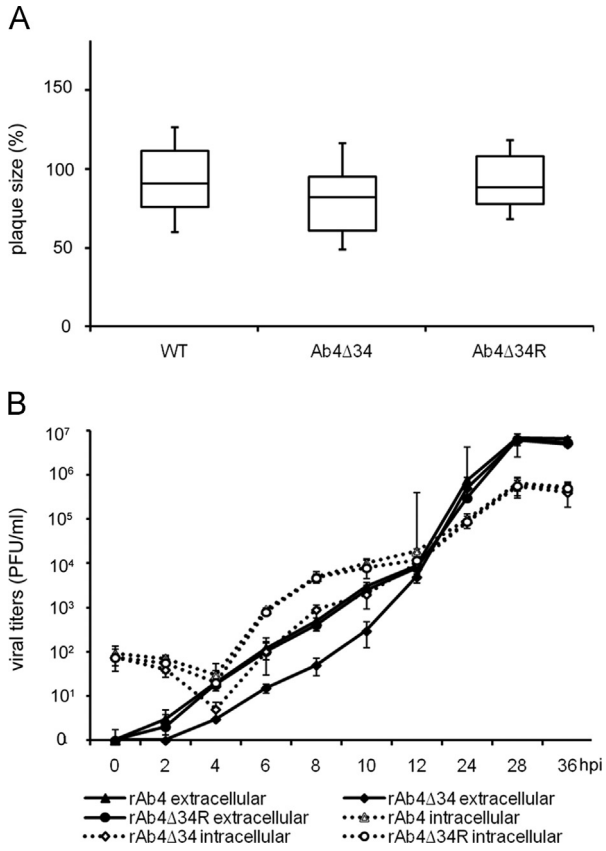

Fig. 9. Single-step growth kinetics and plaque sizes of rAb4Δ34 in comparison with those of parental virus and rAb4_34R. (A) For analysis of plaques sizes, NBL6 cells were infected with parental or mutant viruses and diameters of 50 plaques per virus were measured after 3 days p.i. Plaque sizes are shown as mean plaque diameters obtained in each experiment. Plaque sizes or rAb4 were set at 100%. (B) For analysis of single-step growth kinetics, NBL6 cells were infected with parental, rAb4Δ34 or rAb4Δ34R viruses. Significant differences in the growth properties of the viruses were identified at early (2–10 h p.i), but not late times of infection (12–36 h p.i). Errors bars represent standard deviations.

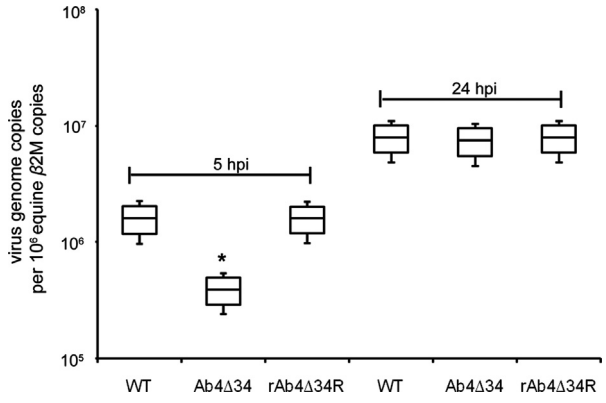

Fig. 10. Replication properties of ORF34-negative virus in PBMC. Isolated equine PBMC were infected with parental, rAb4Δ34 or rAb4Δ34R virus for 5 or 24 h. Virus genome copies in PBMC were determined using qPCR targeting the EHV-1 IR6 (ORF67) gene. The equine β2M gene was used for normalization of virus to host DNA copies. Means of viral genome copies normalized to 1×10^6 β2M copies are shown for the 5 and 24 h time point. Significant differences ($p < 0.05$) are indicated with an asterisk (*). All samples were run in triplicate and errors bars represent standard deviations.

determined by immunoblot analysis is bigger than predicted based on the primary sequence. Our ubiquitin pull-down experiments suggest that the 28-kDa pORF34 moiety represents the viral protein that is linked to a single ubiquitin molecule in the early stages of infection, which may act as a signal for other ubiquitin ligases to attach additional ubiquitin molecules at later times of infection. As a target protein must be marked with at least four or more ubiquitin molecules before it is recognized by the proteasome (Peters et al., 1994; Thrower et al., 2000), the addition of multiple copies of ubiquitin to pORF34 at later times of infection is likely necessary for degradation of pORF34 by the 26S proteasome.

Another interesting finding was that pORF34 was stable until 10 h p.i. and was only degraded after that time. This finding led us to examine whether expression of a late viral gene caused degradation either directly or indirectly. We were able to confirm that treatment of infected cells with PAA, a drug that inhibits expression of late viral proteins, resulted in enhanced stability of pORF34. Our conclusion from the data is that pORF34 stability is dependent on the time after infection and that pORF34 may only be required at early times after infection or that its function at later times after infection requires the protein be modified by ubiquitination.

Immunofluorescence analysis and fractionation studies of infected cells indicated that the ORF34 protein is located in the cytoplasm of infected cells. These findings are in agreement with previous results for the VZV orthologue, which was reported to also be present in the cytosol of infected cells (Reddy et al., 1998). Moreover, examination of the replication properties of an EHV-1 lacking ORF34 (rAb4Δ34) revealed a significant reduction of one-step growth kinetics and virus genome copies when compared to those of rAb4 and rAb4Δ34R. This was true both for equine fibroblast cells and equine PBMC at early but not late times after infection.

Taking all data presented in this study into consideration, we conclude that EHV-1 pORF34 (i) is expressed with early kinetics, (ii) localizes to the cytosol of virus-infected cells, (iii) is stable during early stages of infection but is degraded from its amino-terminus through the ubiquitin/proteasome pathway, an activity that is mediated directly or indirectly by late viral gene products, and (iv) is required for efficient virus growth *in vitro* at early stages of infection. Further studies will be performed to address, which late protein(s) of EHV-1 are involved in the degradation of pORF34 and which residues in the protein are required for this activity. The role of the ORF34 gene product as well as the biological consequences of its degradation *in vivo* will be investigated.

Materials and methods

Virus and cells

Mutant viruses were based on EHV-1 wild type strain Ab4. All genetic manipulations and virus reconstitutions were done using the infectious bacterial artificial chromosome (BAC) clone pAb4, in which mini-F vector sequences also contain the gene expressing the enhanced green fluorescence protein (eGFP) instead of ORF71 that encodes gp2 (Rudolph et al., 2002). Rabbit kidney (RK13) cells were propagated in modified Eagle's medium (MEM) (Biochrom) supplemented with 5% fetal bovine serum (FBS) (Biochrom), 100 U/ml penicillin, and 100 μg/ml streptomycin (1% penicillin–streptomycin). Equine dermal (NBL-6) cells were grown in Iscove's modified Dulbecco's medium (IMDM; Invitrogen) supplemented with 20% FBS and 1% penicillin–streptomycin. Peripheral blood mononuclear cells (PBMC) were isolated from heparinized blood collected from healthy horses by density gradient centrifugation over Biocoll separating solution (density 1.077 g/ml) following the manufacturer's instructions (Biochrom). After two washing steps, cells were resuspended in RPMI 1640 supplemented with 10% FBS, 0.3 mg/ml glutamine, 100 μg/ml kanamycin, nonessential amino acids (Biochrom) and 1% penicillin–streptomycin.

Antibodies

Anti-peptide polyclonal pORF34-specific antibodies targeting amino- or carboxy-terminal sequences were commercially generated (Genscript). The peptides were selected according to hydrophilicity plots and their sequences are given in Table 1. The anti-HA tag (6E2) mouse monoclonal antibody (MAb) and rabbit anti-β-actin polyclonal antibody (pAb) were purchased from Cell Signaling Technologies. MAb FK2 recognizing mono- and poly-ubiquitin was obtained from Enzo Life Sciences. Mouse anti-EHV-1 gM MAb F6 (Ma et al., 2012; Rudolph and Osterrieder, 2002; Said et al., 2012) and EHV-1 gB MAb 3F6 were described before (Allen and Yeargan, 1987; Neubauer et al., 1997). Anti-6X His epitope tag rabbit pAb was purchased from Rockland. Alexa Fluor 568-conjugated goat anti-mouse and Alex Fluor 488 goat anti-rabbit IgG were obtained from Invitrogen, horseradish peroxidase-conjugated goat anti-rabbit and goat anti-mouse antibodies purchased from Southern Biotech.

Plasmids

The EHV-1 ORF34 gene was amplified by PCR using primers P1 and P2 (Table 2). The PCR products were digested with *Bam*HI and *Eco*RI and inserted into pcDNA3 (Invitrogen) resulting in recombinant plasmid pcDNA_34. To construct pcDNA_34Kan, the kanamycin resistance *aphAI* (kan^R) gene was amplified from plasmid pEPkan-S by PCR using primers P3 and P4 (Table 2). The amplified kan^R gene was cloned into a *ClaI* site located within ORF34. To generate pcDNA3 resulting in HA tag (YPYDVPDYA) expression at the C-terminus of ORF34 (pcDNA_34-HA), the ORF34 gene was amplified by PCR from Ab4 strain of EHV-1 using primers P1 and P5, the latter containing sequences encoding the HA tag (Table 2). The 6XHis (pMT107)-tagged ubiquitin expression plasmid has been previously described and was kindly provided by Dr. Mathias Treier, EMBL, Heidelberg, Germany (Treier et al., 1994).

BAC cloning and mutagenesis

For all genetic manipulations, *Escherichia coli* (*E. coli*) strain GS1783 harboring a temperature-sensitive Red recombination system and a gene encoding the endonuclease *I-SceI* in its genome was used. GS1783 cells containing pAb4 were maintained in Luria-Bertani (LB) medium containing 30 μg/ml chloramphenicol. Deletion of ORF34 was done by two-step Red recombination exactly as described before (Tischer et al., 2006) and using PCR primers P8 and P9 (Table 2) that allowed replacement of ORF34 by the *aph*AI (kan^R) gene amplified from plasmid pEPKan-S. Kanamycin-resistant colonies were isolated and screened by PCR and restriction fragment length polymorphism (RFLP) to detect *E. coli* cells harboring mutant clones. The final construct, pAb4Δ34, was obtained after removal of the *aph*AI gene. To create pAb4 with HA tag sequences fused to the C-terminus of ORF34 (pAb4_34-HA), we designed primers P10 and P11 (Table 2). Finally, to reintroduce the authentic ORF34 in pAb4Δ34, a PCR fragment containing EHV-1 ORF34 was cloned into pcDNA3 using the restriction enzymes *BamHI* and *EcoRI*. Then kan^R sequences were cloned into the *ClaI* site, which is located at nucleotide position 184–189 bp of ORF34. The revertant pAb4Δ34R was finalized by removal of *aph*AI as described above using primers P12 and P13 (Table 2). PCR, RFLP, and nucleotide sequencing using primers P6 and P7 (Table 2) confirmed the genotypes of the mutant and revertant pAb4 clones.

Reconstitution of recombinant viruses

To produce wild-type recombinant (r)Ab4, its derivative with a deletion in ORF34 (rAb4Δ34) or a recombinant with an HA-tagged ORF34 protein (rAb4_34-HA), RK13 cells were transfected with 2 μg of BAC DNA. Transfection was performed as previously described (Rudolph et al., 2002).

Southern blotting

Southern blotting was used to confirm the deletion of ORF34 in pAb4Δ34. DNA of pAb4, pAb4Δ34 or pAb4Δ34R was digested with

Table 1
Synthetic pORF34 peptides for production of polyclonal antibodies.

Peptide name	Amino acid sequence	Amino acid residues
N-pORF34	MDSPRGISTATGDAC	1–15
C-pORF34	WMANYCIPDLDEHAD	146–160

Table 2
Oligonucleotides used in this study.

Primer	Product	Sequence 5′–3′
Plasmid		
P1	ORF34	*att***ggatcc**gccaccatggattctccacgcggtatct
P2	in pcDNA3	*acc***gaattc**tcaatccgcgtgttcgtcgaggt
P3	ORF34+aphAI	*cct***atcgat**acggacgatctgctggagat<u>aggatgacgacgataagtaggg</u>
P4	inpCDNA3	*tta***atcgat**agcatctaggccatcacccc<u>caaccaattaaccaattctgattag</u>
P5	ORF34+HA in pcDNA3	gaa***gaattc***tcaagcgtaatctggaacatcgtatgggtaatccgcgtgttcgtcgag
Sequencing and probe		
P6	Sequencing and	tagagttgacgcttcctctt
P7	Southern blot	aactaacaataaatacatac
Mutagenesis		
P8	ORF34 deletion	tgctctcgccgctcctgtgttagcgtatactgcccaagaataaaaaagcaaaaaataa ac <u>aggatgacgacgataagtaggg</u>
P9		acgtatataaactaaaaattgtttatttttgctttttttattcttgggcagtatacgcta<u>caaccaattaaccaattctgattag</u>
P10	HA tag insertion	ggccaactactgcatccctgacctcgacgaacacgcggattacccatacgatgtt ccagattacgcttgataaaaaagca<u>aggatgacgacgataagtaggg</u>
P11		tatataaactaaaaattgtttatttttgctttttatcaagcgtaatctggaacatcgtat gggtaatccgcgtgttc<u>gcaaccaattaaccaattctgattag</u>
Revertant		
P12	ORF34+aphAI	tgctctcgccgctcctgtgttagcgtatactgcccaagaaatggattctccacgcggtat
P13		acgtatataaactaaaaattgtttatttttgctttttatcaatccgcgtgttcgtcg

– Restriction enzyme sites are given in lower case bold letters; sequences in italics indicate additional bases, which are not present in the EHV-1 sequence.
– Underlined sequences indicate the template-binding region of the primers for PCR amplification with pEPkan-s.

XbaI and the fragments separated by 0.8% agarose gel electrophoresis. DNA was then transferred onto a positively charged nylon membrane and hybridized using a digoxigenin-labeled ORF34 probe (Table 2) generated using the PCR DIG Probe Synthesis Kit (Roche) as previously described (Osterrieder et al., 1996; Ziegler et al., 2005). Hybridization was detected with an anti-digoxigenin alkaline phosphatase (AP) antibody (Roche) and bound antibody conjugates were visualized by chemiluminescence (CDP-Star, Roche).

Immunoblotting and immunoprecipitation

For Western blot analysis, RK13 cells were seeded in 6-well plates that were either mock-infected or infected with the various viruses as indicated. Pellets of infected cells were resuspended in radioimmunoprecipitation assay (RIPA) buffer (1 mM Tris, pH 7.4, 1% Triton X-100, 0.25% sodium deoxycholate, 5 M sodium chloride, 0.5 mM EDTA, 0.1% sodium dodecyl sulfate [SDS]) and a protease inhibitor cocktail (Roche). Samples were mixed with sample loading buffer (1 M Tris–HCl, pH 6.8, 0.8% SDS, 0.4% glycerol, 0.15% β-mercaptoethanol, 0.004% bromophenol blue), heated at 65 °C for 5 min, and subjected to SDS-10% polyacrylamide gel electrophoresis (PAGE) exactly as described before (von Einem et al., 2007). Expression of EHV-1 ORF34 protein (pORF34), and glycoprotein M (gM) or cellular β-actin was detected with specific antibodies and peroxidase conjugates listed earlier. Reactive bands were visualized by enhanced chemiluminescence (ECL plus, GE Healthcare). To examine pORF34 phosphorylation, cell lysates were treated with λ-protein phosphatase (λ-PPase; New England BioLabs) for 30 min at 30 °C before electrophoresis as described (Ma et al., 2012; Said et al., 2012).

For immunoprecipitation, RK13 cells were first transfected with the 6XHis (pMT107)-tagged ubiquitin expression plasmid for 24 h, then infected with recombinant rAb4_34-HA. Pellets of transfected and infected cells were resuspended in RIPA buffer and insoluble material was removed by centrifugation at 2500*g* for 2 min. The supernatant was incubated with either the anti-HA or anti-His MAb by shaking gently at 4 °C overnight and the complexes were then precipitated using protein G-agarose (Thermo Scientific) for 2 h. Immune complexes were pelleted, washed in RIPA buffer 3 times, and heated at 65 °C for 5 min in loading buffer as described (Cohen and Seidel, 1995; Feng et al., 2004). Reactive bands were visualized by detection using ECL after SDS–PAGE and immunobloting with the reciprocal antibodies. For precipitation of ubiquitinated pORF34 from cells infected with rAb4 or rAb4_34HA virus, immunoprecipitation was performed as described above using the anti-ubiquitin MAb or the anti-HA MAb, respectively. After separation by SDS–PAGE, proteins were transferred to PVDF membranes and visualized after immunobloting exactly as described above using polyclonal anti-C-pORF34 antibodies.

Determination of the kinetic class of EHV-1 ORF34

To determine the kinetics of ORF34 expression, NBL-6 cells were either mock-infected or infected with parental or rAb4_34-HA viruses at a multiplicity of infection (m.o.i) of 5 in the presence of the viral DNA synthesis inhibitor phosphonoacetic acid (PAA; Sigma) at a concentration of 300 μg/ml, followed by incubation in fresh medium containing PAA for 24 h (Honess and Watson, 1977; Said et al., 2012). In order to differentiate between IE and E gene expression, NBL6 cells were infected with rAb4_34-HA in the presence of cycloheximide (CX; Sigma) at a concentration of 100 μg/ml medium, which is known to inhibit viral protein synthesis in EHV-1 infected cells and to allow accumulation of EHV-1 IE mRNA (Khattar et al., 1995; Said et al., 2012). After 5 h, cells were extensively washed and incubated with fresh medium containing the transcription inhibitor actinomycin D (Act-D; Sigma) at 5 μg/ml. Translation of accumulated IE mRNA is possible after wash-out of cycoheximide, while Act-D prevents further transcription of mRNA. Cells were analyzed after each treatment by immunoblot analysis.

Protein stability

In order to assess the effect of time after infection on pORF34 stability, RK13 cells were infected with rAb4_34-HA at an m.o.i. of 1 before samples were harvested at the indicated time points (1, 2, 3, 4, 5, 6, 8, 10, 12, 16 and 24 h p.i.) and analyzed using Western blotting.

To determine whether pORF34 is modified post-translationally by glycosylation, PNGaseF and EndoH treatment of infected-cell lysates was performed as previously described (Seyboldt et al., 2000). Cell lysates were suspended in digestion buffer and digested with PNGaseF or EndoH as recommended by the manufacturer (BioLab). The reaction was mixed and incubated for 3 h at 37 °C. Separation of reaction products was examined by Western blotting using anti-C-pORF34 antibody (Table 1).

To determine the degradation pathway of pORF34, rAb4_34-HA-infected RK13 cells were incubated with medium containing the proteasome inhibitor lactacystin at a final concentration of 10 mM (Parkinson et al., 1999) added for 24 h at 37 °C after a 1 h virus adsorption period. Infected cells were then collected and lysed, and cell lysates analyzed by Western blot. To determine whether proteasomal degradation of the protein was ubiquitin-dependent, RK13 cells were transfected with the 6XHis (pMT107)-tagged ubiquitin expression plasmid for 24 h and then infected with rAb4_34-HA. Treatment with the proteasome inhibitor for 24 h followed, before infected cells were lysed, immunoprecipitated, and subjected to Western blot analysis as described above. Moreover, RK13 cells were also treated with the E1 inhibitor Pyr-41 (Sigma) used at a final concentration of 25 μM of for 8 h prior to infection, exactly as previously described (Teale et al., 2009; Yang et al., 2007). Following pre-treatment, inhibitors were removed by washing the cells with PBS and cells were infected with rAb4_34-HA virus (m.o.i.=5). After 1 h of infection, cells were treated again with Pyr-41 for 24 h, then the treated cells were harvested and analyzed by Western blotting.

Indirect immunofluorescence (IF) and cell fractionation

To evaluate intracellular expression of pORF34 in infected cells by indirect IF, NBL6 cells were grown on coverslips and infected with either parental, rAb4_34-HA or rAb4Δ34 viruses at an m.o.i of 0.1. At 16 h p.i., cells were fixed with 2% paraformaldehyde in PBS for 10 min and washed with PBS 3 times, followed by permeabilization with 0.1% saponin for 30 min. After blocking with 2% bovine serum albumin for 1 h, cells were incubated with anti-HA mouse MAb (1/500) or anti-ORF34 pAb (1/200) for 1 h at RT. After 3 washing steps with PBS, cells were incubated with secondary Alexa Fluor 568 goat anti-mouse or Alexa Fluor 488 goat anti-rabbit (1/5000) IgG for 1 h at RT exactly as described previously (Ahn et al., 2011; Ma et al., 2012). Finally, after 3 washing steps, Vectashield® mounting medium with DAPI (Vector Laboratories) was added to cells and the coverslips were inspected under a Zeiss Axio Imager M1 microscope (Zeiss, Germany).

Cells were separated into cytoplasmic and nuclear fractions by the following procedure (Ahn et al., 2011; de Mendez et al., 1994). NBL6 cells were infected with rAb4_34-HA and washed at 24 h p.i with ice-cold PBS. Cells were then scraped off of the surface, centrifuged and pellets resuspended in ice-cold buffer (10 mM HEPES, pH 7.9; 10 mM $MgCl_2$; 10 mM KCl; 0.5 mM DTT). Cells were disrupted and centrifuged at 300*g* for 5 min at 4 °C to pellet the nuclei. The supernatant was saved as the cytoplasmic fraction. Nuclear pellets were disrupted with RIPA buffer and centrifuged at

3000*g* for 15 min at 4 °C to pellet insoluble debris. Cytoplasmic and nuclear fractions were analyzed by Western blotting.

Virus growth kinetics, plaque size measurements and quantitative PCR (qPCR)

Plaque sizes and growth kinetics of rAb4Δ34 were determined and compared to parental virus (von Einem et al., 2007). For plaque size measurements, confluent monolayers of NBL6 cells were infected with mutant and parental virus and plaque sizes were determined by IF at 3 days p.i. and analyzed using ImageJ software (http://rsb.info.nih.gov/ij/). For single-step growth kinetics, NBL6 cells were infected with mutant and parental viruses at an m.o.i. of 3. Single-step growth curves were determined in three independent experiments by titrating cell culture supernatants or from cell lysates generated by freeze–thawing twice (cell-associated titers) at the indicated times p.i. (Rudolph et al., 2002).

To determine whether the deletion of ORF34 would affect virus replication in equine PBMC, quantitative (q) PCR was used. Equine PBMC (2×10^7 cells) were infected either with parental rAb4, rAb4Δ34 or rAb4_34-HA viruses at an m.o.i of 0.5. After EHV-1 infection, cells were treated with citrate buffer (pH 3.0) to inactivate remaining extracellular virus (Mettenleiter, 1989; van Der Meulen et al., 2000) and fresh culture media was added before cells were incubated at 37 °C for either 5 or 24 h. For qPCR, PBMC were washed three times with PBS to remove viruses in the supernatant, and genomic DNA was extracted by using an RTP® DNA/RNA Virus Mini Kit (Stratec AG). qPCR was then performed by using the 7500-Fast real-time qPCR system (Applied Biosystems) in a total volume of 20 μl (Goodman et al., 2007). The horse β2-microglobulin (β2M) gene was used to normalize virus to host genome copies using primers and an MGB probe as described earlier (Goodman et al., 2006, 2007). pAb4 was used as the virus standard and a BAC clone of equine chromosome containing the β2M gene (kindly provided by Dr D. Antczak, Cornell University, NY, USA) was used for host genome copy quantification. The experiment was performed in three independent replicates and each sample was also tested in duplicate for each experiment.

Statistical analysis

Using Microsoft Excel, Student's *t*-test for paired data was used to test for significant differences. Data given are means and bars show standard deviations.

Acknowledgments

This work was supported by unrestricted funds from the Freie Universität Berlin to N.O. and in part by scholarship from the Egyptian Ministry of Education to A.S.

References

Ahn, B.C., Kim, S., Zhang, Y., Charvat, R.A., O'Callaghan, D.J., 2011. The early UL3 gene of equine herpesvirus-1 encodes a tegument protein not essential for replication or virulence in the mouse. Virology 420, 20–31.

Allen, G.P., Kaatz, G.W., Rybak, M.J., 2004. *In vitro* activities of mutant prevention concentration-targeted concentrations of fluoroquinolones against Staphylococcus aureus in a pharmacodynamic model. Int. J. Antimicrob. Agents 24, 150–160.

Allen, G.P., Yeargan, M.R., 1987. Use of lambda gt11 and monoclonal antibodies to map the genes for the six major glycoproteins of equine herpesvirus 1. J. Virol. 61, 2454–2461.

Boutell, C., Sadis, S., Everett, R.D., 2002. Herpes simplex virus type 1 immediate-early protein ICP0 and is isolated RING finger domain act as ubiquitin E3 ligases *in vitro*. J. Virol. 76, 841–850.

Bregegere, F., Milner, Y., Friguet, B., 2006. The ubiquitin–proteasome system at the crossroads of stress-response and ageing pathways: a handle for skin care? Ageing Res. Rev. 5, 60–90.

Carroll, C.L., Westbury, H.A., 1985. Isolation of equine herpesvirus 1 from the brain of a horse affected with paresis. Aust. Vet. J. 62, 345–346.

Caughman, G.B., Staczek, J., O'Callaghan, D.J., 1985. Equine herpesvirus type 1 infected cell polypeptides: evidence for immediate early/early/late regulation of viral gene expression. Virology 145, 49–61.

Cohen, J.I., Seidel, K.E., 1995. Varicella-zoster virus open reading frame 1 encodes a membrane protein that is dispensable for growth of VZV *in vitro*. Virology 206, 835–842.

Crabb, B.S., Studdert, M.J., 1995. Equine herpesviruses 4 (equine rhinopneumonitis virus) and 1 (equine abortion virus). Adv. Virus Res. 45, 153–190.

Davison, A.J., Eberle, R., Ehlers, B., Hayward, G.S., McGeoch, D.J., Minson, A.C., Pellett, P.E., Roizman, B., Studdert, M.J., Thiry, E., 2009. The order herpesvirales. Arch. Virol. 154, 171–177.

de Mendez, I., Garrett, M.C., Adams, A.G., Leto, T.L., 1994. Role of p67-phox SH3 domains in assembly of the NADPH oxidase system. J. Biol. Chem. 269, 16326–16332.

Demartino, G.N., Gillette, T.G., 2007. Proteasomes: machines for all reasons. Cell 129, 659–662.

Dye, B.T., Schulman, B.A., 2007. Structural mechanisms underlying posttranslational modification by ubiquitin-like proteins. Annu. Rev. Biophys. Biomol. Struct. 36, 131–150.

Everett, R.D., 2000. ICP0, a regulator of herpes simplex virus during lytic and latent infection. Bioessays 22, 761–770.

Feng, P., Scott, C.W., Cho, N.H., Nakamura, H., Chung, Y.H., Monteiro, M.J., Jung, J.U., 2004. Kaposi's sarcoma-associated herpesvirus K7 protein targets a ubiquitin-like/ubiquitin-associated domain-containing protein to promote protein degradation. Mol. Cell. Biol. 24, 3938–3948.

Forster, A., Hill, C.P., 2003. Proteasome degradation: enter the substrate. Trends Cell Biol. 13, 550–553.

Goodman, L.B., Loregian, A., Perkins, G.A., Nugent, J., Buckles, E.L., Mercorelli, B., Kydd, J.H., Palu, G., Smith, K.C., Osterrieder, N., Davis-Poynter, N., 2007. A point mutation in a herpesvirus polymerase determines neuropathogenicity. PLoS Pathog. 3, e160.

Goodman, L.B., Wagner, B., Flaminio, M.J., Sussman, K.H., Metzger, S.M., Holland, R., Osterrieder, N., 2006. Comparison of the efficacy of inactivated combination and modified-live virus vaccines against challenge infection with neuropathogenic equine herpesvirus type 1 (EHV-1). Vaccine 24, 3636–3645.

Gray, W.L., Baumann, R.P., Robertson, A.T., Caughman, G.B., O'Callaghan, D.J., Staczek, J., 1987. Regulation of equine herpesvirus type 1 gene expression: characterization of immediate early, early, and late transcription. Virology 158, 79–87.

Hershko, A., Ciechanover, A., 1998. The ubiquitin system. Annu. Rev. Biochem. 67, 425–479.

Honess, R.W., Watson, D.H., 1977. Herpes simplex virus resistance and sensitivity to phosphonoacetic acid. J. Virol. 21, 584–600.

Kalejta, R.F., Shenk, T., 2003. Proteasome-dependent, ubiquitin-independent degradation of the Rb family of tumor suppressors by the human cytomegalovirus pp71 protein. Proc. Nat. Acad. Sc.i U.S.A. 100, 3263–3268.

Khattar, S.K., van Drunen Littel-van den Hurk, S., Babiuk, L.A., Tikoo, S.K., 1995. Identification and transcriptional analysis of a 3′-coterminal gene cluster containing UL1, UL2, UL3, and UL3.5 open reading frames of bovine herpesvirus-1. Virology 213, 28–37.

Ma, G., Feineis, S., Osterrieder, N., Van de Walle, G.R., 2012. Identification and characterization of equine herpesvirus type 1 pUL56 and its role in virus-induced downregulation of major histocompatibility complex class I. J. Virol. 86, 3554–3563.

McDowell, M.E., Purushothaman, P., Rossetto, C.C., Pari, G.S., Verma, S.C., 2013. Phosphorylation of Kaposi's sarcoma-associated herpesvirus processivity factor ORF59 by a viral kinase modulates its ability to associate with RTA and oriLyt. J. Virol. 87, 8038–8052.

McGeoch, D.J., Cunningham, C., McIntyre, G., Dolan, A., 1991. Comparative sequence analysis of the long repeat regions and adjoining parts of the long unique regions in the genomes of herpes simplex viruses types 1 and 2. J. Gen. Virol. 72 (Pt 12), 3057–3075.

McGeoch, D.J., Dalrymple, M.A., Davison, A.J., Dolan, A., Frame, M.C., McNab, D., Perry, L.J., Scott, J.E., Taylor, P., 1988. The complete DNA sequence of the long unique region in the genome of herpes simplex virus type 1. J. Gen. Virol. 69 (Pt 7), 1531–1574.

Mettenleiter, T.C., 1989. Glycoprotein gIII deletion mutants of pseudorabies virus are impaired in virus entry. Virology 171, 623–625.

Neubauer, A., Beer, M., Brandmuller, C., Kaaden, O.R., Osterrieder, N., 1997. Equine herpesvirus 1 mutants devoid of glycoprotein B or M are apathogenic for mice but induce protection against challenge infection. Virology 239, 36–45.

Nugent, J., Birch-Machin, I., Smith, K.C., Mumford, J.A., Swann, Z., Newton, J.R., Bowden, R.J., Allen, G.P., Davis-Poynter, N., 2006. Analysis of equid herpesvirus 1 strain variation reveals a point mutation of the DNA polymerase strongly associated with neuropathogenic *versus* nonneuropathogenic disease outbreaks. J. Virol. 80, 4047–4060.

O'Callaghan, D.J., Osterrieder, N., 2008. Herpesviruses of horses. Encycl. Virol. 2, 411–420 (third ed.).

Oster, B., Bundgaard, B., Hupp, T.R., Hollsberg, P., 2008. Human herpesvirus 6B induces phosphorylation of p53 in its regulatory domain by a CK2- and p38-independent pathway. J. Gen. Virol. 89, 87–96.

Osterrieder, N., Neubauer, A., Brandmuller, C., Kaaden, O.R., O'Callaghan, D.J., 1996. The equine herpesvirus 1 IR6 protein influences virus growth at elevated temperature and is a major determinant of virulence. Virology 226, 243–251.
Parkinson, J., Lees-Miller, S.P., Everett, R.D., 1999. Herpes simplex virus type 1 immediate-early protein vmw110 induces the proteasome-dependent degradation of the catalytic subunit of DNA-dependent protein kinase. J. Virol. 73, 650–657.
Peters, J.M., Franke, W.W., Kleinschmidt, J.A., 1994. Distinct 19 S and 20 S subcomplexes of the 26 S proteasome and their distribution in the nucleus and the cytoplasm. J. Biol. Chem. 269, 7709–7718.
Pickart, C.M., Fushman, D., 2004. Polyubiquitin chains: polymeric protein signals. Curr. Opin. Chem. Biol. 8, 610–616.
Prosch, S., Priemer, C., Hoflich, C., Liebenthaf, C., Babel, N., Kruger, D.H., Volk, H.D., 2003. Proteasome inhibitors: a novel tool to suppress human cytomegalovirus replication and virus-induced immune modulation. Antivir. Ther. 8, 555–567.
Reddy, S.M., Cox, E., Iofin, I., Soong, W., Cohen, J.I., 1998. Varicella-zoster virus (VZV) ORF32 encodes a phosphoprotein that is posttranslationally modified by the VZV ORF47 protein kinase. J. Virol. 72, 8083–8088.
Rudolph, J., O'Callaghan, D.J., Osterrieder, N., 2002. Cloning of the genomes of equine herpesvirus type 1 (EHV-1) strains KyA and racL11 as bacterial artificial chromosomes (BAC). J. Vet. Med. B: Infect. Dis. Vet. Public Health 49, 31–36.
Rudolph, J., Osterrieder, N., 2002. Equine herpesvirus type 1 devoid of gM and gp2 is severely impaired in virus egress but not direct cell-to-cell spread. Virology 293, 356–367.
Said, A., Azab, W., Damiani, A., Osterrieder, N., 2012. Equine herpesvirus type 4 UL56 and UL49.5 proteins downregulate cell surface major histocompatibility complex class I expression independently of each other. J. Virol. 86, 8059–8071.
Said, A., Osterrieder, N., 2013. Equine herpesvirus type 1 (EHV-1) open reading frame 59 encodes an early protein that is localized to the cytosol and required for efficient virus growth. Virology 449, 263–269.
Seyboldt, C., Granzow, H., Osterrieder, N., 2000. Equine herpesvirus 1 (EHV-1) glycoprotein M: effect of deletions of transmembrane domains. Virology 278, 477–489.
Soboll Hussey, G., Hussey, S.B., Wagner, B., Horohov, D.W., Van de Walle, G.R., Osterrieder, N., Goehring, L.S., Rao, S., Lunn, D.P., 2011. Evaluation of immune responses following infection of ponies with an EHV-1 ORF1/2 deletion mutant. Vet. Res. 42, 23.
Teale, A., Campbell, S., Van Buuren, N., Magee, W.C., Watmough, K., Couturier, B., Shipclark, R., Barry, M., 2009. Orthopoxviruses require a functional ubiquitin–proteasome system for productive replication. J. Virol. 83, 2099–2108.
Telford, E.A., Watson, M.S., McBride, K., Davison, A.J., 1992. The DNA sequence of equine herpesvirus-1. Virology 189, 304–316.
Telford, E.A., Watson, M.S., Perry, J., Cullinane, A.A., Davison, A.J., 1998. The DNA sequence of equine herpesvirus-4. J. Gen. Virol. 79 (Pt 5), 1197–1203.
Thrower, J.S., Hoffman, L., Rechsteiner, M., Pickart, C.M., 2000. Recognition of the polyubiquitin proteolytic signal. EMBO J. 19, 94–102.
Tischer, B.K., von Einem, J., Kaufer, B., Osterrieder, N., 2006. Two-step red-mediated recombination for versatile high-efficiency markerless DNA manipulation in *Escherichia coli*. Biotechniques 40, 191–197.
Treier, M., Staszewski, L.M., Bohmann, D., 1994. Ubiquitin-dependent c-Jun degradation *in vivo* is mediated by the delta domain. Cell 78, 787–798.
van Der Meulen, K.M., Nauwynck, H.J., Buddaert, W., Pensaert, M.B., 2000. Replication of equine herpesvirus type 1 in freshly isolated equine peripheral blood mononuclear cells and changes in susceptibility following mitogen stimulation. J. Gen. Virol. 81, 21–25.
von Einem, J., Smith, P.M., Van de Walle, G.R., O'Callaghan, D.J., Osterrieder, N., 2007. *In vitro* and *in vivo* characterization of equine herpesvirus type 1 (EHV-1) mutants devoid of the viral chemokine-binding glycoprotein G (gG). Virology 362, 151–162.
Yang, Y., Kitagaki, J., Dai, R.M., Tsai, Y.C., Lorick, K.L., Ludwig, R.L., Pierre, S.A., Jensen, J.P., Davydov, I.V., Oberoi, P., Li, C.C., Kenten, J.H., Beutler, J.A., Vousden, K.H., Weissman, A.M., 2007. Inhibitors of ubiquitin-activating enzyme (E1), a new class of potential cancer therapeutics. Cancer Res. 67, 9472–9481.
Ziegler, C., Just, F.T., Lischewski, A., Elbers, K., Neubauer, A., 2005. A glycoprotein M-deleted equid herpesvirus 4 is severely impaired in virus egress and cell-to-cell spread. J. Gen. Virol. 86, 11–21.